Disassembling and Bleaching of Chloride-Free *pharaonis* Halorhodopsin by Octyl-β-glucoside

Megumi Kubo,[‡] Maki Sato,[‡] Tomoyasu Aizawa,[‡] Chojiro Kojima,[§] Naoki Kamo,[||] Mineyuki Mizuguchi,[⊥] Keiichi Kawano,[‡] and Makoto Demura*,[‡]

Division of Biological Sciences, Graduate School of Science, Hokkaido University, 060-0810, Japan, Laboratory of Biophysics, Graduate School of Biological Sciences, Nara Institute of Science and Technology, 8916-5 Takayama, Ikoma, Nara 630-0192, Japan, Graduate School of Pharmaceutical Sciences, Hokkaido University, Sapporo 060-0812, Japan, and Faculty of Pharmaceutical Sciences, Toyama Medical and Pharmaceutical University, Toyama 930-0194, Japan

Received June 13, 2005; Revised Manuscript Received July 29, 2005

ABSTRACT: *Natronomonas* (*Natronobacterium*) *pharaonis* halorhodopsin (NpHR) is a transmembrane, seven-helix retinal protein of the archaeal bacterium and acts as an inward light-driven chloride ion pump in the membrane. The denaturation process of NpHR solubilized with *n*-octyl-β-D-glucopyranoside (OG) was investigated to clarify the effects of the chloride ion and pH on the stability and bleaching of the NpHR chromophore. Initially, active NpHR solubilized with *n*-dodecyl-β-D-maltopyranoside (DM) was obtained from the recombinant halo-opsin (NpHO), which was expressed in *Escherichia coli* cells, by adding all-*trans* retinal to the medium. Apparent molecular weight of the active NpHR solubilized with DM, which was determined by gel-filtration chromatography and dynamic light scattering, indicated the oligomeric state. The bleaching of NpHR in the dark by the addition of 50 mM OG in the presence and absence of chloride was investigated. In the presence of 256 mM NaCl, the bleaching of NpHR was strongly inhibited. On the other hand, in the absence of NaCl, an immediate decrease of absorbance at 600 nm was observed. Stopped-flow rapid-mixing analysis clarified the bleaching process in the absence of chloride as DM−NpHR (oligomeric) ↔ OG−NpHR (disassembled) ↔ intermediate → NpHO and free retinal, and each rate constant were determined. The formation of an intermediate (450 nm) in the dark was found to be strongly dependent on pH, as well as anion and detergent concentrations. The disassembling and protonation of a Schiff base corresponding to the bleaching intermediate is also discussed.

Halorhodopsin (HR),[1] bacteriorhodopsin (bR), sensory rhodopsin I, and phoborhodopsin (sensory rhodopsin II) are transmembrane, seven-helix retinal proteins in the membrane of the archaeal bacterium (*1*). These four proteins have the same global fold, and an all-*trans* retinal chromophore binds to a conserved lysine residue on the seventh helix via a protonated Schiff base. bR (an outward-directed, light-driven proton pump) has become one of the most typical model systems for studying the membrane protein structure, folding, bioenergetics, photochemistry, and mechanism of proton transport (*2*, *3*).

On the other hand, HRs (an inward-directed, light-driven chloride ion pump) from *Halobacterium salinarum* (*4*, *5*) and *Natronomonas* (*Natronobacterium*) *pharaonis* (*6*, *7*) alone have been extensively studied; however, several HRs have been identified and reported (*8*−*10*). In 2000, the crystalline structure of the *H. salinarum* HR (HsHR) determined at 1.8 Å resolution had been reported (*11*). Because the primary structures of HsHR and *N. pharaonis* HR (NpHR) are very highly homologous (66%) (*12*), their tertiary structures would be expected to be conserved. One of the greatest advantages of using NpHR is its stability, which is higher than that of HsHR in a chloride-free system. In addition, an *Escherichia coli* expression system for the archaeal retinal proteins including NpHR was recently reported (*13*, *14*). In this expression system, the use of a histidine-tagged protein rendered it possible to purify the retinal proteins in only one step, thereby allowing simple and large-scale preparation (*15*−*17*). In the case of recombinant NpHR purified from *E. coli* membrane, the visible circular dichroism (CD) exciton coupling corresponding to the self-assembling structure having a two-dimensional crystalline is observed to be the same as that purified from the *N. pharaonis* membrane.

The HsHR during the dark and light adaptations in NaCl contains about 45 and 75% all-*trans* configuration (*18*). In Na_2SO_4, there is no adaptation, and the all-*trans* content of the sample was shown to be approximately 67% (*19*). In contrast, in NpHR, the all-*trans* content of the preparation is known to remain constant at 85% under all conditions tested (different salts and light illumination) (*7*, *19*). The photocycle of NpHR has intermediates analogous to those of bR (*20*). However, in the photocycle of NpHR, no intermediate corresponding to the M (deprotonated Schiff

* To whom correspondence should be addressed. Telephone/fax: +81-11-706-2771. E-mail: demura@sci.hokudai.ac.jp.
[‡] Graduate School of Science, Hokkaido University.
[§] Nara Institute of Science and Technology.
[||] Graduate School of Pharmaceutical Sciences, Hokkaido University.
[⊥] Toyama Medical and Pharmaceutical University.

[1] Abbreviations: DM, *n*-dodecyl-β-D-maltopyranoside; OG, *n*-octyl-β-D-glucopyranoside; NpHR, halorhodopsin from *Natrononomas pharaonis*; HsHR, halorhodopsin from *Halobacterium salinarum*.

10.1021/bi0511235 CCC: $30.25
Published on Web 09/03/2005

base) is thought to exist (*6*). More recently, the roles played by putative anion-binding sites in the cytoplasmic and extracellular channels of NpHR have been investigated using the wild-type protein and various mutant proteins, all of which were functionally expressed in *E. coli* cells (*21*).

The thermal and photobleaching of bR and/or retinal-binding process from the apoprotein without a retinal (opsin) have been previously investigated in terms of the effects of light, ion species, temperature, pH, and detergents (*2*, *22*−*25*). In these experiments, the self-assembling states of bR have typically been monitored using visible CD spectroscopy. It is thought that, in the solubilized state and under light illumination, the purple membrane is disassembled into a monomeric state by *n*-octyl-*β*-D-glucopyranoside (OG); moreover, the stability of the membrane is considered to be much lower than that of the native structure (*24*). On the other hand, the process of retinal binding from bacterio-opsin to the intermediates in the detergent micelles has been reported from the visible absorption shift (*2*). However, to date, there has been no comparative study of the stability and refolding of the HR in detergent micelles.

In this paper, the denaturation process of *N. pharaonis* HR (NpHR) solubilized with OG was investigated to clarify the effects of the presence of chloride ion and pH on the stability and bleaching of the NpHR chromophore. We expressed histidine-tagged wild-type NpHR in *E. coli* cells and elucidated the reversible intermediate between the native and denaturized (bleached) structures in a nonionic detergent, OG, using stopped-flow rapid mixing. As mentioned above, NpHR and HsHR exhibit slight differences in stability in a chloride-free system, as well as in terms of light−dark adaptation and anion selectivity for pumping. Thus, it remains important to clarify the stability and assembly of NpHR under solubilized conditions. Gel-filtration chromatography and dynamic light-scattering (DLS) methods were also applied to measure the apparent molecular weight (*26*, *27*). On the basis of these experiments, the transient intermediate and changes in the number of associated NpHR molecules during the bleaching process are discussed below.

MATERIALS AND METHODS

Protein Expression and Purification of NpHR. The expression of the recombinant NpHR in *E. coli* [strain BL21 (DE3)] and purification procedures have been described previously (*15*). Fractions of the proteins separated with Ni-NTA-agarose (Qiagen, Hilden, Germany) were collected by elution (flow rate, 56 mL/h) with buffer A [50 mM Tris-HCl (pH 7.0), 300 mM NaCl, 150 mM imidazole, and 0.1% *n*-dodecyl-*β*-D-maltopyranoside (dodecyl maltoside, DM) (Dojindo Lab, Kumamoto, Japan)]. The samples were stored at 4 °C for 1 month, and then the supernatant (DM−NpHR complex) was collected by centrifugation (18000*g*, 20 min).

Preparation of the Anion-Deleted DM−NpHR Complex. The anion-deleted blue species of NpHR ($NpHR^{blue}$) were prepared by replacing buffer A with buffer B [10 mM 2-morpholinopropanesulfonic acid, MOPS (pH 7.0), and 0.1% DM] by passage over Sephadex-G 25 in a PD-10 column (8.3 mL; Amersham Pharmacia Biotech, Uppsala, Sweden) at a flow rate of 2 mL/min. After buffer exchange, the protein concentration was estimated using an excitation coefficient ϵ_{600} of 50 000 M^{-1} cm^{-1} (*28*).

Gel-Filtration Chromatography of the DM−NpHR Complex. Superdex 200 pg resin (Amersham Biosciences, Hilden, Germany) was applied to a chromatography column (inner diameter, 1.5 cm; height, 75 cm). The DM−NpHR complex was eluted (flow rate, 1 mL/3 min) with buffer [10 mM NaP_i (pH 8.0), 150 mM NaCl, and 0.1% DM]. The fractions were collected in a volume of 0.5−1.0 mL for each tube. The reference materials for the calibration curves were Blue Dextran 2000 (Amersham Biosciences, Hilden, Germany), which was used to determine the void volume and check the column packing, as well as several known standard substances, i.e., those in the Pharmacia Gel Filtration Kit [Thyroglobulin (MW 669 000), Ferritin (MW 440 000), and Catalase (MW 232 000), Amersham Biosciences, Hilden, Germany] and Albumin (MW 66 000), Ovalbumin (MW 44 000), and Chymotrypsinogen A (MW 13 700) (Sigma, St. Louis, MO). Fresh Blue Dextran 2000 solution (1.0 mg/mL) was prepared in the eluent buffer. The proper combination of standard substances was dissolved in the eluent buffer. The concentration of each protein ranged between 5 and 20 mg/mL (except for Ferritin, 1 mg/mL). The volume of these calibration solutions was 1−2% of the total gel bed volume (V_t). A calibration curve of K_{av} values versus log molecular weight was prepared according to the instruction manual. The K_{av} of each protein was calculated according to the following equation, $K_{av} = (V_e - V_o)/(V_t - V_o)$, where V_e is the elution volume for the protein and V_o is the column void volume, which is equal to the elution volume for Blue Dextran 2000. The absorbance of each fraction was measured using a Nanodrop ND-1000 spectrophotometer (NanoDrop Technologies, Inc., Rockland, DE) (path length, 1 mm).

DLS Measurements. The molecular mass of the DM micelle and the solubilized NpHR in DM was examined by DLS using DynaPro (Protein Solutions, Charlottesville, VA) at 20 °C. The buffer containing 0.1% DM, 10 mM MOPS (pH 7), NaCl (∼100 mM−1 M) with and without 45 μM NpHR was centrifuged at 10 000 rpm for 10 min. The intensity of light (780 nm) scattered at an angle of 90° was measured. The measurement of the intensity of the light was repeated at least 10 times. The data were analyzed on the basis of the hydrodynamic radius, assuming that the particles were spherical and of standard density, using Dynamics 4.0 and DynaLS software, as described by Osawa et al. (*27*).

Time-Resolved Absorption Measurements. Time-resolved absorption changes caused by the manual mixing of chloride-free $NpHR^{blue}$ with OG were measured with a HITACHI U-2000 spectrophotometer (Hitachi, Tokyo, Japan) after the samples were mixed for 20 s in the 300−700 nm region at 25 °C using a single accumulation and a scanning speed of 800 nm/min. The measuring medium was buffer B, which contained various concentrations of NaCl. The path length of the optical cuvette was 10 mm. In the pH titration experiment, 10 mL of 6-Mix buffer [citric acid, MES, MOPS, Tricine, CHES, and CAPS] containing 0.1% DM was used.

Time-resolved absorption changes caused by the rapid mixing of chloride-free $NpHR^{blue}$ with OG were measured using an RA-2000 stopped-flow spectrophotometer (Otsuka Electronics, Osaka, Japan) with a dead time of 1.3 ms. The path length of the optical cell was 10 mm. The ratio of the mixing volumes of the protein and the 100 mM OG solutions was 1:1. The final concentrations of protein and OG were 4

μM and 50 mM, respectively. Rapid scan absorption changes in the 340−660 nm range were measured using a photodiode array at 1-s intervals after mixing, which gave the difference spectra caused by the addition of OG until 256 s after mixing. Singular value decomposition (SVD) treatment (*29*) was performed to determine the number of spectral components, as well as to remove the noise. Kinetic analysis and a global fitting were performed using the Igor Pro 3.14 software package (Wave Metrics, Lake Oswego, OR) (*17*).

Extraction of Retinal from NpHR and High-Performance Liquid Chromatography (HPLC) Analysis. After the addition of 50 mM OG to the NpHR samples for 0 s, 50 s, 30 min, and 3 h, the extraction of the retinal from the NpHR samples was carried out as described by Shimono and co-workers (*30*). A total of 100 μL of the samples was mixed with 300 μL of 90% methanol and 50 μL of 1 M hydroxylamine. After denaturation, retinal oxime was extracted by adding 800 μL of hexane under conditions of vigorous mixing. The emulsion was centrifuged with a hand-rotating centrifuge, and 50−200 μL of the upper phase was immediately separated by HPLC. A silica column (6 × 150 mm, YMC-0123, Yamamura, Japan) was used for HPLC with 12% (v/v) ethyl acetate and 0.12% (v/v) ethanol in hexane as a solvent at a flow rate of 1.0 mL/min, and the oximes were detected at 360 nm. All reagents were HPLC-grade reagents. The molar compositions of the retinal isomers were calculated from the areas of the peaks in the HPLC patterns. The extinction coefficients of all-*trans* and 13-*cis* retinaloximes (*31*) and that of the free retinal obtained in this study were used to estimate retinal composition. Assignment of the peaks was performed by comparing the peaks with those in the HPLC pattern from retinal oximes extracted by the same method from bR kept in the dark.

RESULTS

Estimation of the Apparent Molecular Weight of the DM−NpHR Complex. The purified NpHR on the Ni-NTA affinity column and the reference proteins for the calibration of molecular weight were fractionated by gel-filtration chromatography in the presence of 150 mM NaCl. The absorbance of these fractionations was observed at 280 and 578 nm (Figure 1). The absorbance at 578 nm could be attributed to the functional NpHR. On the other hand, the absorbance at 280 nm signified the total protein. The linear calibration was obtained as shown in the inset in Figure 1. The NpHR sample was separated into two peaks in elution volumes of 52 (void volume) and 63 mL when the absorbance was observed at 280 nm. In regard to the main peak (elution volume, 63 mL), absorbance at 578 nm was observed. This leads to a highly pure NpHR preparation with a ratio of 1.28 between an OD at 280 and 578 nm; these results agreed well with the reported value (1.25) for the purified NpHR obtained from the *N. pharaonis* membrane (*28*). Sodium dodecyl sulfate−polyacrylamide gel electrophoresis (SDS−PAGE) of these fractionations by this chromatographic approach was performed to confirm the molecular weight of the denatured proteins. A major band on SDS−PAGE with a mass of approximately 32 kDa was detected for both of the two peaks obtained with elution volumes of 52 and 63 mL (data not shown). These results suggest that the fractions eluted earlier were *pharaonis* halo-opsin (*p*HO), which does not retain a retinal inside the protein and is inactive. Nonreduced SDS−PAGE was also performed, because the NpHR has three cysteine residues. The results were identical to those obtained by SDS−PAGE under reduced conditions. Thus, it was concluded that the aggregation of the DM−NpHO complex was not ascribable to an intermolecular disulfide bond.

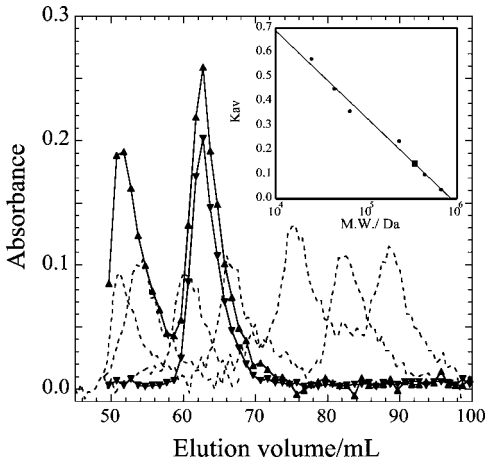

FIGURE 1: Absorbance at 280 nm (▲) and 578 nm (▼) of fractions collected by gel-filtration chromatography. The dotted lines show the absorbance at 280 nm of Blue Dextran 2000 and protein standards. (Inset) The calibration curve using the globular protein standards (●) on Superdex 200 pg. The apparent molecular weight of the DM−NpHR complex (■) was estimated by substituting K_{av}, which was calculated from the elution volume (V_e) for the calibration curve.

On the basis of the calibration of the apparent molecular weight of the eluted protein and the elution volume of each protein applied to this column (inset of Figure 1), the K_{av} of each protein was calculated (see the Materials and Methods). The K_{av} value of the main peak indicated that the apparent molecular weight of the DM−NpHR complex was approximately 340 kDa, which is larger than the molecular weight of the NpHR monomer (32 kDa). Moreover, the apparent molecular weight of the DM−NpHR complex and the DM micelles according to the DLS method was 400−430 and 66−100 kDa, under the assumption that the monomodal particles were spherical. Therefore, these results suggested the oligomeric state of the NpHR in the DM micelle system. This result was supported from previous reports of the visible CD exciton coupling, corresponding to the self-assembling structure having a two-dimensional crystalline (*15, 21*).

Bleaching of DM−NpHR by OG in the Presence and Absence of the Chloride Ion. Figure 2 shows the change in the relative absorbance of chloride-free DM−NpHR^{blue} at λ_{max} (600 nm) after the addition of 0−50 mM OG at 25 °C in the dark. In the absence of OG, chloride-free DM−NpHR^{blue} did not exhibit a rapid decrease in absorbance. When DM−NpHR^{blue} was resolubilized to a 10 mM OG solution, the absorbance of NpHR^{blue} decreased; moreover, when DM−NpHR^{blue} was resolubilized to a concentration of more than 25 mM OG, it exhibited almost total bleaching within 1 h. These results were in agreement with the critical micelle concentration (cmc; 22 mM) of OG (*32*). Thus, we adopted a concentration of 50 mM OG in the following experiments. Interestingly, as shown in Figure 2, a biphasic denaturation curve in the absorbance at the initial resolubilizing step of NpHR from DM to OG micelle system was observed within 20 s when concentrations of OG exceeding

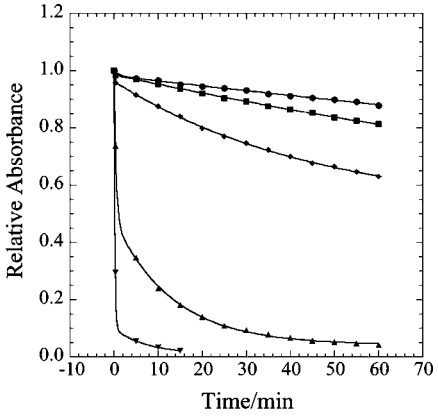

FIGURE 2: Changes in the relative absorbance at the maximum difference in the absorbance of chloride-free NpHR with the addition of 0 (●), 5 (■), 10 (◆), 25 (▲), and 50 (▼) mM OG. The wavelengths measured were 635, 620, 620, 600, and 600 nm, respectively. The concentration of NpHR was 4 μM. The final solution in the sample contained 0−50 mM OG, 2 mM DM, and 10 mM MOPS (pH 7.0).

10 mM were used. Decreasing the light scattering of the oligomeric DM−NpHR might have led to this result.

The bleaching of DM−NpHR by the addition of 50 mM OG in the presence and absence of chloride was also investigated as time-resolved absorption changes in the 300−700 nm region (Figure 3). These spectra were measured before the addition of OG and from 30 s to 1 h after the addition of OG. In the presence of 256 mM NaCl (Figure 3C), a small discrete change at the initial step and a subsequent slight decrease were observed. A similar degree of stability of NpHR in the presence of more than 64 mM NaCl was observed and is shown in Figure 4. These findings indicate that the bleaching of NpHR induced by the addition of OG was strongly inhibited by the local structure of the chromophore, which has a chloride-binding site. In the presence of 32 mM NaCl (Figure 3B), a gradual decrease in absorption at 580 nm and a concomitant increase in absorption at 380 nm were observed within this period of measurement. These two peaks did not indicate an unequivocal isosbestic point. However, in the absence of NaCl (Figure 3A), an immediate decrease initiated at 600 nm and an increase at 380 nm were observed. In addition, two isosbestic points were observed at 420 and 505 nm, as well as a broad peak between these isosbestic points, thereby suggesting the presence of a structural intermediate.

Structural Intermediate Obtained by the Bleaching of Chloride-Free NpHR^{blue}. To measure the spectral changes of chloride-free DM−NpHR^{blue} in the early stages after the addition of OG, a stopped-flow rapid-mixing technique was applied. Figure 5A shows a two-dimensional contour map of the spectral changes between 350 and 650 nm as a function of time after the addition of 50 mM OG. The interval used for measurement was 1 s. As shown in this figure, when chloride-free DM−NpHR^{blue} with a visible absorption at 600 nm was resolubilized with OG, the absorption peak at 380 nm was generated with a maximum peak at 450 nm. This result agrees with the detection of two isosbestic points (Figure 3A). Thus, it was concluded that, by the addition of OG, the chloride-free DM−NpHR^{blue} decreases as follows:

$$\text{DM}-\text{NpHR}^{\text{blue}} \rightarrow \text{I}_{450} \rightarrow \text{I}_{380} \qquad (1)$$

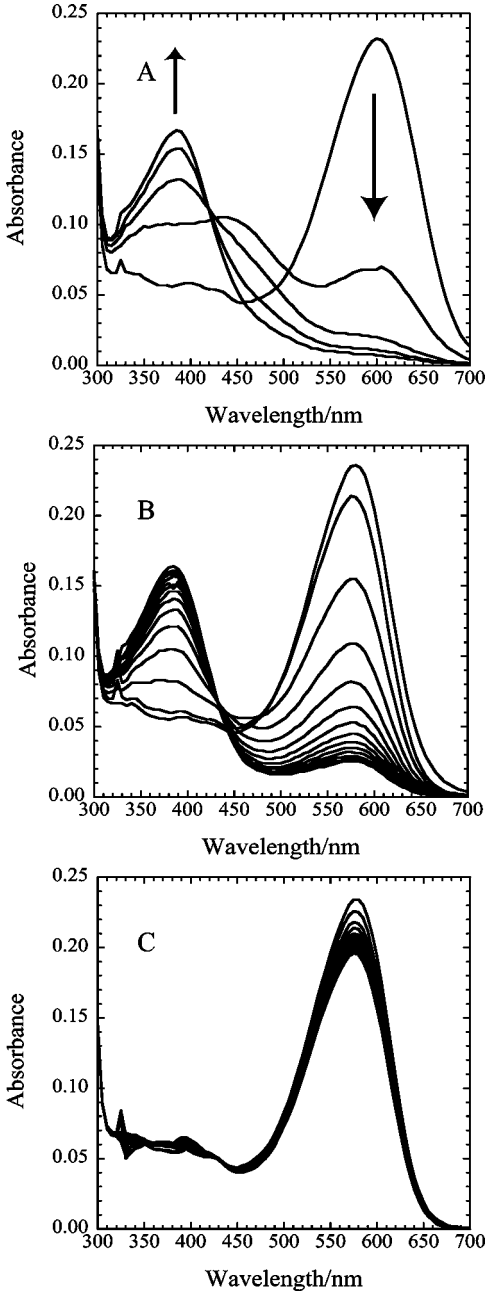

FIGURE 3: Changes in the absorption spectra of NpHR during the bleaching reaction by the addition of 50 mM OG at pH 7. The concentrations of NaCl were 0 mM (A), 32 mM (B), and 256 mM (C). The first spectrum obtained before the addition of OG, the second spectrum obtained after the addition of OG at 30 s, and the following spectra obtained in 5-min intervals until 1 h are shown. Noise was obtained in the region near 325 nm because of a change in the stray light-cutting filter used in the spectrometer. The final solution in the sample contained 50 mM OG, 2 mM DM, and 10 mM MOPS.

As mentioned above, it was found that the DM−NpHR is in the oligomeric state, and the addition of excess OG led to a discrete decrease in absorption as a result of a decrease in light scattering because of disassembling of the oligomeric state. In addition, we could observe a small decrease of the negative exciton band (600 nm) of visible CD spectrum at the beginning of exchange of DM and excess OG micelles, which corresponds to the intermolecular exciton coupling of NpHR chromophores (data not shown), suggesting disruption of the NpHR oligomer. Therefore, the reaction in

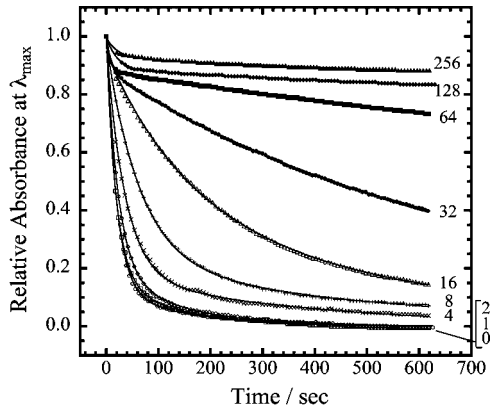

FIGURE 4: Decay curves of relative absorbance during the bleaching of NpHR at the λ_{max}. The numbers signify the concentration of chloride contained in each sample. NaCl concentrations, λ_{max}, and the identifiers are 0 mM (600 nm), ○; 1 mM (600 nm), □; 2 mM (600 nm), ◇; 4 mM (595 nm), × ; 8 mM (585 nm), +; 16 mM (580 nm), △; 32 mM (580 nm), ●; 64 mM (580 nm), ■; 128 mM (580 nm), ◆; and 256 mM (580 nm), ▲, respectively. The solid lines are the calculated curves. The conditions used for the sample solution were the same as those described in the caption of Figure 3.

eq 1 can be modified as follows:

$$\mathrm{DM{-}(NpHR^{blue})}_m \rightarrow \mathrm{OG{-}(NpHR^{blue})}_n \rightarrow \mathrm{I_{450}} \rightarrow \mathrm{I_{380}} \quad (2)$$

where subscripts m and n ($m > n$) denote the number of NpHR monomers in the assembly. Kinetic analysis of the two-dimensional contour map of the spectral changes was performed by a combination of the singular-value decomposition (SVD) approach and the global-fitting approach using a multiexponential function. On the basis of this analysis, three optimal rate constants, i.e., 0.114, 0.048, and 0.005 s^{-1}, were determined. Figure 5B shows the calculated two-dimensional contour map drawn by three-exponential fitting using the optimal rate constants. Figure 6 shows the curve fitting of absorbance changes at 600, 450, and 380 nm using these three rate constants. This fitting indicates that decreases from chloride-free $NpHR^{blue}$ to I_{450} and an increase from I_{450} to I_{380} were dominant, because the fraction of the fastest rate constant, 0.114 s^{-1}, which was attributed to the decrease in the assembling number of components for assembly between $DM{-}(NpHR^{blue})_m$ and $OG{-}(NpHR^{blue})_n$, accounted for only 5% of the total change at 600 nm. Thus, the medium and the lowest rate constants (i.e., 0.048 and 0.005 s^{-1}) were attributed to the formation of I_{450} and I_{380}, respectively.

Effects of Chloride and pH on the Bleaching of NpHR. It was found that the bleaching kinetics of NpHR because of the addition of OG depends upon the concentration of the chloride ion, as shown in Figures 3 and 4. This finding indicates that the equilibrium, chloride-bound NpHR ⇔ chloride-free NpHR, should be introduced for chloride-dependent bleaching. When the chloride concentration was higher than the chloride dissociation constant of NpHR (K_d = ~5 mM), there was a small amount of chloride-free NpHR. In this case, the transient I_{450} did not accumulate, and thus, the formation of I_{380} was slower than that of chloride-free NpHR (0.005 s^{-1}). When there was no chloride in the detergent system, all chloride-free NpHR changed to I_{380} through an I_{450} intermediate, as shown in eq 2.

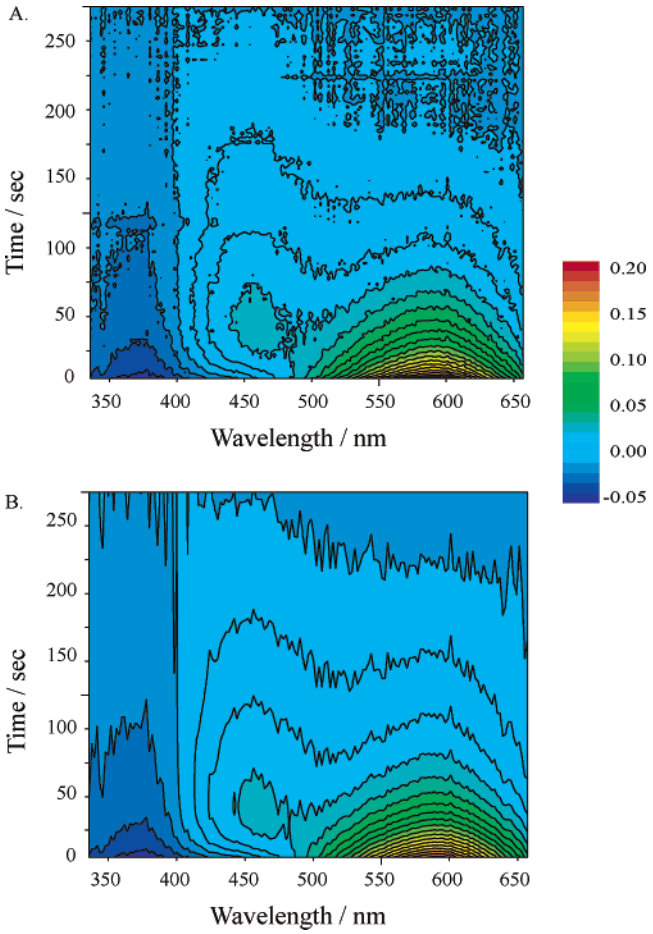

FIGURE 5: Observed (A) and calculated (B) two-dimensional contour maps of differential absorbance during the bleaching reaction of chloride-free DM−NpHR obtained from stopped-flow rapid-mixing experiments. The sampling interval and the total observation times were 1 and 250 s, respectively. Differential absorbance [Abs (t) − Abs (250 s)] was plotted. The calculated map was obtained from three-exponential fitting after the SVD analysis and the global fitting. The contour intervals of ΔAbs were 0.01. The final concentration of the mixed solution was 50 mM OG, 1 mM DM, and 10 mM MOPS (pH 7.0).

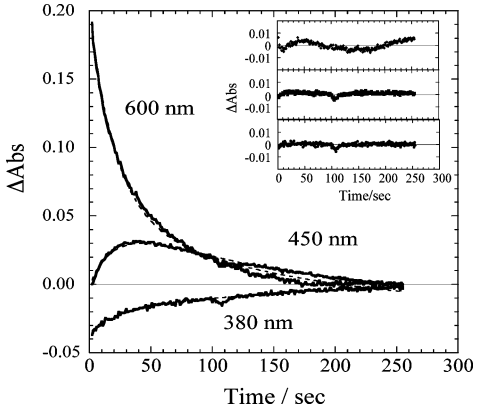

FIGURE 6: Absorption change at three wavelengths (380, 450, and 600 nm) based on the results shown in parts A and B of Figure 5 obtained during the bleaching reaction of NpHR in the absence of NaCl. The solid and broken lines show the observed and global-fitted data, respectively. The inset represents the residuals between the best-fit and the observed data.

On the other hand, to clarify the effects of pH on the bleaching process of NpHR, the spectral changes in NpHR by the addition of OG were measured at pH 1.5 (Figure 7).

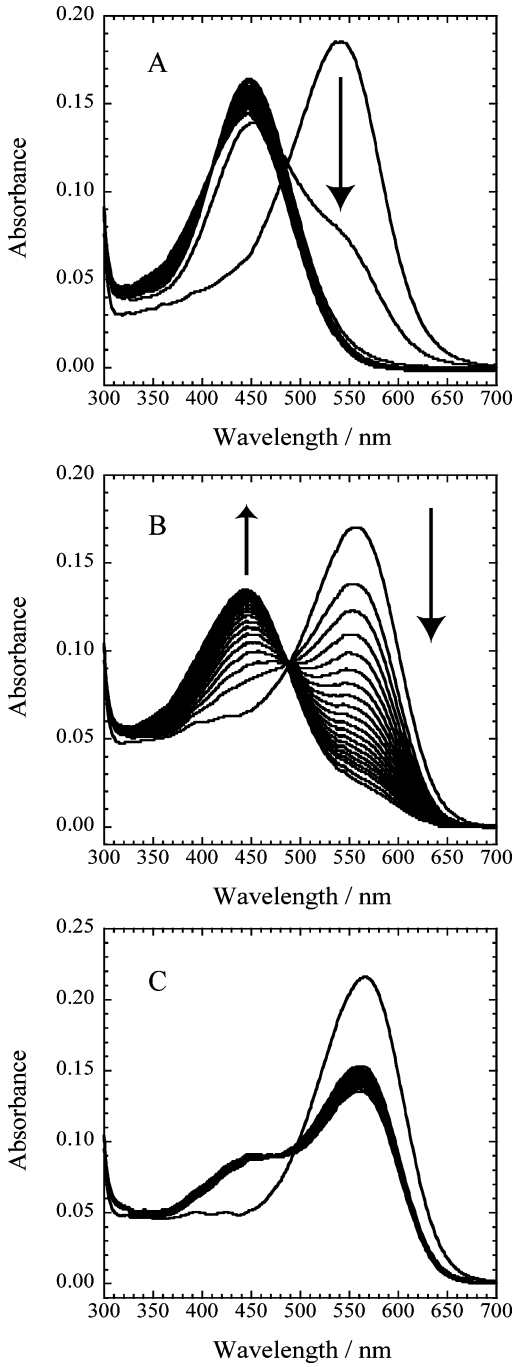

FIGURE 7: Change in the absorption spectra of NpHR during the bleaching reaction by the addition of 50 mM OG at pH 1.5. The concentrations of NaCl were 0 mM (A), 32 mM (B), and 256 mM (C). The first spectrum obtained before the addition of OG, the second spectrum obtasined after the addition of OG at 30 s, and the following spectra obtained in 5-min intervals until 1 h are shown. The final solution in the sample contained 50 mM OG, 2 mM DM, and 10 mM 6-Mix buffer. The pH was adjusted with H_2SO_4.

When the pH is changed from 7 to 1.5, the λ_{max} of chloride-free NpHR largely blue-shifted from 600 to 542 nm (Figure 7A). This absorbance at a low pH remained stable for at least 2 h. The addition of 50 mM OG to the chloride-free NpHR at the low pH induced a rapid decrease in absorbance at the λ_{max} (542 nm) and a subsequent increase in absorption at 450 nm as well as the appearance of absorption (450 nm) at a neutral pH. Similarly, the rate of increase at 450 nm was reduced by the presence of the chloride anion (parts A−C of Figure 7). However, it was clear that the production of acidic I_{450} was strongly inhibited, which was in contrast to the transient formation of I_{450} of the chloride-free NpHR at a neutral pH (Figure 2), suggesting that the bleaching process that occurs between I_{450} and I_{380} may be inhibited by the protonation of NpHR. When the acidic I_{450} was neutralized in the absence of chloride, the recovery of $NpHR^{blue}$ (600 nm) and the formation of I_{380} were observed at the same time.

Table 1: Ratio of the Retinal Isomer Compositions of Several Samples during the Bleaching Process by the Addition of OG in the Dark

	retinal isomer composition (%)		
	retinaloxime forms[a]		
sample	all-*trans*	13-*cis*	retinal forms[a]
$NpHR^{blue}$ (NaCl free)	89	9	2
I_{450} (50 s)[b]	87	10	3
yellow species (30 min)[b]	57	9	35
yellow species (3 h)[b]	43	9	49

[a] Retinaloxime and retinal forms were extracted in the dark with and without hydroxylamine by the denaturation treatment with organic solvent (see the Materials and Methods). [b] Incubation time with 50 mM OG.

Isomerization and Binding of the Retinal to the Protein. The retinal isomer composition of various NpHR samples was analyzed using HPLC; the results are shown in Table 1. The retinaloximes were produced by the cleavage of Schiff-base bonds by the reaction with hydroxylamine (*30*−*33*). Four isomers of retinaloximes identified as all-*trans* (15-*syn*, 15-*anti*) and 13-*cis* (15-*syn*, 15-*anti*) were detected. Four similar isomers have been detected when the retinal was cleaved from *pharaonis* phoborhodopsin (*33*). The HPLC elution pattern of these retinaloximes extracted from chloride-free $NpHR^{blue}$ was similar to that of NpHR in the presence of NaCl. After the addition of 50 mM OG to the chloride-free $NpHR^{blue}$ for 0, 50 s, 30 min, and 3 h, retinal cleavage and an extraction treatment were carried out. These incubation times corresponded to those of $NpHR^{blue}$, I_{450}, at the initial stage of the yellow species (380 nm pigment) and to the latter stages of the yellow species (380 nm pigment), respectively. As shown in Table 1, the composition of the retinal isomers of $NpHR^{blue}$ and I_{450} did not change. This provided evidence that the large blue shift of λ_{max} from 600 to 450 nm in the dark was not the result of the isomerization of the retinal, e.g., in the case of the 9-*cis* configuration, which has been detected in deionized bR in a pink membrane under continuous illumination (*34*). Similarly, retinaloximes were extracted from the I_{450} trapped at a low pH, suggesting that the retinal isomerization of acidic I_{450} in the dark and its covalent binding as a Schiff base are similar to those of the native structure (data not shown). In contrast, the yellow species exhibited fewer all-*trans* retinaloxime forms and more nonretinaloxime forms, i.e., when extracted from NpHR samples without hydroxylamine using only the organic solvent with incubation time, which might be attributed to the presence of the free retinal.

DISCUSSION

Bacteriorhodopsin and halorhodopsin exhibit two-dimensional crystal packing in the lipidic phase. The crystal structure of *Halobacterium salinarum* HR (HsHR), which

is highly homologous to the NpHR used in the present study, has a trimeric structure as the fundamental assembling unit (*11*). In the present study, active recombinant NpHR was successfully expressed in *E. coli* cells and was purified in the solubilization state with a mild detergent, *n*-dodecyl-*β*-D-maltopyranoside (DM). The apparent molecular weight of the DM−NpHR estimated by gel-filtration chromatography was 340 kDa, suggesting the assemblage of NpHR monomers in the DM micelles. Using the apparent molecular weight of DM−NpHR, the association number of NpHR monomers contained in a single complex was estimated by various methods. The molecular weight of the NpHR monomer is 32 000 Da according to ESI mass spectrometry (*14*). Using this value, the number of NpHR monomers was calculated to be 10.6. The molecular weight of a single DM micelle is 75 600 Da, and the aggregation number of DM is 148 (*35*). If the DM−NpHR complex were to be assembled together as one DM micelle, the number of NpHR monomers would be expected to be 8.3, although it is difficult to estimate the accurate amount of the DM complex. It is known that the visible CD spectrum of NpHR solubilized with DM detergent indicates a bilobe pattern because of the intermolecular exciton coupling of NpHRs (*15*, *28*). On the other hand, discrete decreases in light scattering at the initial stage of OG mixing were observed (Figure 2). Similarly, it has been reported that solubilized HsHR obtained from the *H. salinarum* membrane has a single positive CD band in the visible region when 0.5% OG is used (*36*). These findings additionally suggest a decrease in the association number of NpHR monomers in the OG micelle system.

The present study was the first to demonstrate, as based on the resolubilization of the DM−NpHR by the addition of OG detergent, that the chloride-free $NpHR^{blue}$ species (600 nm) bleached to the yellow species (I_{380}) by way of an intermediate (I_{450}) at neutral pH. However, the formation of intermediate I_{450} was strongly inhibited by the chloride-binding of NpHR, and yellow species I_{380} was also blocked by the protonation of NpHR. The distribution of the released retinal in the OG-resolubilized NpHR was identified using extraction with an organic solvent and cleavage of the Schiff base by reaction with hydroxylamine. In the absence of chloride, the ratio of the free retinal increased during the last half of the bleaching process (Table 1), which was released from the Schiff base of NpHR. However, the intermediate species (I_{450}), which was generated transiently at a neutral pH, did not lead to an increase in free retinals released from the Schiff base. In addition, the all-*trans*/13-*cis* isomerization ratio before and after the resolubilization of NpHR by the addition of OG detergent was the same.

The bleaching and retinal binding of bR has been reported under both dark and light conditions. In the case of photobleaching of the purple membrane by OG detergent, the primary absorbance showed a direct change to a yellow species (380 nm); moreover, the structural intermediate with a λ_{max} of approximately 450 nm was not observed (*24*). On the other hand, under dark conditions, the structural intermediate of bR, I_{440}, has been observed during the denaturation process by the addition of an anionic detergent, SDS (*37*). The stability of this intermediate at pH 5 was higher than that at a neutral pH. This observation is thus similar to the characteristics of I_{450} of NpHR observed in the present study. In a previous study, it was concluded that this I_{440} of bR would be expected to exhibit a loosely folded protein structure. The formation rate constant and the wavelength at the isosbestic point are both similar to those of NpHR. Although the types of detergents used in these studies differed in terms of being anionic or nonionic, the characteristics of these results nonetheless appeared to be similar. Previously, similar absorption spectra for recombinant wild-type bR in DMPC/CHAPS/SDS-mixed micelles at an acidic pH were observed (*38*). At pH 1.9, the absorption spectra of bR displayed a transition to a species with a λ_{max} at 442 nm in the absence of NaCl. That study concluded that this conversion represents the formation of a free protonated Schiff base (PSB) because of the denaturation of the protein. In contrast, in the presence of 2 M NaCl, a main peak with a λ_{max} at 566 nm was observed at pH 1.9. The results of that experiment suggested that anions can stabilize the PSB of the folded protein by electrostatic interactions. In our study, the visible CD spectra of NpHR−I_{450} did not produce exciton coupling. However, the exciton coupling of NpHR could be slightly recovered, even when the $NpHR^{blue}$ was reconstituted from the acidic I_{450} by neutralization. These results suggest that the I_{450} of the NpHR oligomer has loose packing around the retinal instead of ordered intermolecular interactions, resulting in the formation of a free PSB just like that of bR in the mixed micelles; however, it should be noted that there was a slight λ_{max} difference between the acidic intermediates of bR and NpHR.

It has been reported that bR (*39*−*42*) contains a 9-*cis* retinal under continuous illumination when it is transformed at low pH or in the deionized state. These species exhibit absorption at approximately 430−490 nm as is the case with the bleaching intermediate (I_{450}) of chloride-free NpHR. However, this NpHR intermediate was produced under conditions of nonillumination. As shown in Table 1, it was found that the bleaching intermediate (I_{450}) of chloride-free NpHR contains all-*trans* and 13-*cis* retinals. In addition, a comparison of the reference (*31*) in terms of the HPLC elution pattern of retinaloxime isomers (all-*trans*-, 7-*cis*-, 9-*cis*-, 11-*cis*-, and 13-*cis*-retinals *syn*- and *anti*-oximes) with that of the bleached NpHR in the dark concluded that the bleaching intermediate (I_{450}) of chloride-free NpHR did not contain a 9-*cis* retinal. Investigation of whether NpHR−I_{450} exhibits photoactivity is in progress.

In contrast, the process of the retinal binding of bacterioopsin (bO), which was reconstituted in the model lipid system with an all-*trans* retinal, has been investigated under dark conditions. bR was reconstituted with bO and the all-*trans* retinal by way of the structural intermediates with λ_{max} values of 380 and 440 nm (*22*, *42*, *43*). These intermediates that occur during the retinal-binding process are apparently similar to those observed in our study. However, the previous study concluded that the retinal-binding intermediate (I_{440}) was constituted with the noncovalently bound retinal, because the bR mutant with a substitution for Lys-216 at the retinal-binding site had a similar absorption maximum at 440 nm (*22*). In our study, it was found that the bleaching intermediate of NpHR−I_{450} has a covalently bound retinal, as identified by the HPLC analysis of retinaloximes (Table 1). In addition, NpHR−I_{450} at a low pH reverted to $NpHR^{blue}$ (600 nm species) and rapidly exhibited a visible CD band with exciton coupling by neutralization, as mentioned above. Thus, our

results support the formation of free PSB, even in the NpHR−I_{450} intermediate. Although the I_{450} intermediate of NpHR accumulated because of the addition of OG, the bleaching process that led to the formation of I_{380} from I_{450} strongly inhibited at an acidic pH. On the other hand, at pH 1.5, the absorbance of the chloride-free NpHR without OG (542 nm) was stable, and this pigment gradually red-shifted by addition of chloride (the opposite spectral shift of NpHR at a neutral pH) such as a property of HsHR. There are only two acidic amino acid residues (Asp156 and Asp252) close to the retinal chromophore of NpHR. It is likely that the PSB in the NpHR is highly protected by the local structure that includes these two acidic residues. Future studies will still be needed to clarify the roles played by these residues and to elucidate the effects of the assembly of NpHR on its stability and function.

ACKNOWLEDGMENT

The authors are very grateful to Dr. Kazumi Shimono (Graduate School of Pharmaceutical Sciences, Hokkaido University) and Prof. Katsutoshi Nitta (Graduate School of Science, Hokkaido University) for invaluable discussions and advice.

REFERENCES

1. Spudich, J. L., Yang, C. S., Jung, K. H., and Spudich, E. N. (2000) Retinylidene proteins: Structures and functions from archaea to humans, *Annu. Rev. Cell Dev. Biol. 16*, 365−392.
2. Booth, P. J., Templer, R. H., Curran, A. R., and Allen, S. J. (2001) Can we identify the forces that drive the folding of integral membrane proteins? *Biochem. Soc. Trans*. *29*, 408−413.
3. Váró, G. (2000) Analogies between halorhodopsin and bacteriorhodopsin, *Biophys. Biochem. Acta 1460*, 220−229.
4. Lanyi, J. K. (1990) Halorhodopsin, a light-driven electrogenic chloride-transport system, *Physiol. Rev. 70*, 319−330.
5. Matsuno-Yagi, A., and Mukohata, Y. (1980) ATP synthesis linked to light-dependent proton uptake in a rad mutant strain of *Halobacterium* lacking bacteriorhodopsin, *Arch. Biochem. Biophys. 199*, 297−303.
6. Váró, G., Brown, L. S., Sasaki, H., Kandori, H., Maeda, A., Needleman, R., and Lanyi, J. K. (1995) Light-driven chloride ion transport by halorhodopsin from *Natronobacterium pharaonis*. 1. The photochemical cycle, *Biochemistry 34*, 14490−14499.
7. Váró, G., Needleman, R., and Lanyi, J. K. (1995) Light-driven chloride ion transport by halorhodopsin from *Natronobacterium pharaonis*. 2. Chloride release and uptake, protein conformation change, and thermodynamics, *Biochemistry 34*, 14500−14507.
8. Otomo, J., Tomioka, H., and Sasabe, H. (1992) Properties and the primary structure of a new halorhodopsin from halobacterial strain mex, *Biochim. Biophys. Acta 1112*, 7−13.
9. Soppa, J., Duschl, J., and Oesterhelt, D. (1993) Bacterioopsin, haloopsin, and sensory opsin I of the halobacterial isolate *Halobacterium* sp. strain SG1: Three new members of a growing family, *J. Bacteriol. 175*, 2720−2726.
10. Ihara, K., Umemura, T., Katagiri, I., Kitajima-Ihara, T., Sugiyama, Y., Kimura, Y., and Mukohata, Y. (1999) Evolution of the archaeal rhodopsins: Evolution rate changes by gene duplication and functional differentiation, *J. Mol. Biol. 285*, 163−174.
11. Kolbe, M., Besir, H., Essen, L. O., and Oesterhelt, D. (2000) Structure of the light-driven chloride pump halorhodopsin at 1.8 Å resolution, *Science 288*, 1390−1396.
12. Duschl, A., Lanyi, J. K., and Zimányi, L. (1990) Properties and photochemistry of a halorhodopsin from the haloalkalophile, *Natronobacterium pharaonis*, *J. Biol. Chem. 265*, 1261−1267.
13. Shimono, K., Iwamoto, M., Sumi, M., and Kamo, N. (1997) Functional expression of pharaonis phoborhodopsin in *Escherichia coli*, *FEBS Lett. 420*, 54−56.
14. Hohenfeld, I. P., Wegener, A. A., and Engelhard, M. (1999) Purification of histidine tagged bacteriorhodopsin, pharaonis halorhodopsin, and pharaonis sensory rhodopsin II functionally expressed in *Escherichia coli*, *FEBS Lett. 442*, 198−202.
15. Sato, M., Kanamori, T., Kamo, N., Demura, M., and Nitta, K. (2002) Stopped-flow analysis on anion binding to blue-form halorhodopsin from *Natronobacterium pharaonis*: Comparison with the anion-uptake process during the photocycle, *Biochemistry 41*, 2452−2458.
16. Sato, M., Kikukawa, T., Araiso, T., Okita, H., Shimono, K., Kamo, N., Demura, M., and Nitta, K. (2003) Ser-130 of *Natronobacterium pharaonis* halorhodopsin is important for the chloride binding, *Biophys. Chem. 104*, 209−216.
17. Sato, M., Kikukawa, T., Araiso, T., Okita, H., Shimono, K., Kamo, N., Demura, M., and Nitta, K. (2003) Roles of Ser130 and Thr126 in chloride binding and photocycle of *pharaonis* halorhodopsin, *J. Biochem. 134*, 151−158.
18. Váró, G., Zimányi, L., Fan, X., Sun, L., Needleman, R., and Lanyi, J. K. (1995) Photocycle of halorhodopsin from *Halobacterium salinarium*, *Biophys. J. 68*, 2062−2072.
19. Sato, M., Kubo, M., Aizawa, T., Kamo, N., Kikukawa, T., Nitta, K., and Demura, M. (2005) Role of putative anion-binding sites in cytoplasmic and extracellular channels of *Natronomonas pharaonis* halorhodopsin, *Biochemistry 44*, 4775−4784.
20. Zimányi, L., and Lanyi, J. K. (1997) Fourier transform Raman study of retinal isomeric composition and equilibration in halorhodopsin, *J. Phys. Chem. B 101*, 1930−1933.
21. Lanyi, J. K. (1997) Mechanism of ion transport across membranes. Bacteriorhodopsin as a prototype for proton pumps, *J. Biol. Chem. 272*, 31209−31212.
22. Lu, H., and Booth, P. J. (2000) The final stages of folding of the membrane protein bacteriorhodopsin occur by kinetically indistinguishable parallel folding paths that are mediated by pH, *J. Mol. Biol. 299*, 233−243.
23. Yokoyama, Y., Sonoyama, M., and Mitaku, S. (2004) Inhomogeneous stability of bacteriorhodopsin in purple membrane against photobleaching at high temperature, *Proteins 54*, 442−454.
24. Mukai, Y., Kamo, N., and Mitaku, S. (1999) Light-induced denaturation of bacteriorhodopsin solubilized by octyl-β-glucoside, *Protein Eng. 12*, 755−759.
25. Sasaki, T., Sonoyama, N., Demura, M., and Mitaku, S. (2005) Photobleaching of bacteriorhodopsin solubilized with Triton X-100, *Photochem. Photobiol.*, in press.
26. Guereca, L., and Bravo, A. (1999) The oligomeric state of *Bacillus thuringiensis* Cry toxins in solution, *Biochim. Biophys. Acta 1429*, 342−350.
27. Osawa, M., Tong, K. I., Lilliehook, C., Wasco, W., Buxbaum, J. D., Cheng, H.-Y. M., Penninger, J. M., Ikura, M., and Ames, J. B. (2001) Calcium-regulated DNA binding and oligomerization of the neuronal calcium-sensing protein, calsenilin/DREAM/KChIP3, *J. Biol. Chem. 276*, 41005−41013.
28. Scharf, B., and Engelhard, M. (1994) Blue halorhodopsin from *Natronobacterium pharaonis*: Wavelength regulation by anions, *Biochemistry 33*, 6387−6393.
29. Henry, E. R., and Hofrichter, J. (1992) Singular value decomposition: Application to analysis of experimental data, *Methods Enzymol. 210*, 129−193.
30. Shimono, K., Ikeura, Y., Sudo, Y., Iwamoto, M., and Kamo, N. (2001) Environment around the chromophore in *pharaonis* phoborhodopsin: Mutation analysis of the retinal binding site, *Biophys. Biochem. Acta 1515*, 92−100.
31. Tsukida, K., Ito, M., Tanaka, T., and Yagi, I. (1985) High-performance liquid chromatographic and spectroscopic characterization of stereoisomeric retinaloximes. Improvements in resolution and implication of the method, *J. Chromatogr. 331*, 265−272.
32. Walter, A., Kuehl, G., Barnes, K., and VanderWaerdt, G. (2000) The vesicle-to-micelle transition of phosphatidylcholine vesicles induced by nonionic detergents: Effects of sodium chloride, sucrose, and urea, *Biochim. Biophys. Acta 1508*, 20−33.
33. Imamoto, Y., Shichida, Y., Hirayama, J., Tomioka, H., Kamo, N., and Yoshizawa, T. (1992) Chromophore configuration of *pharaonis* phoborhodopsin and its isomerization on photon absorption, *Biochemistry 31*, 2523−2528.
34. Oesterhelt, D., and Stoeckenius, W. (1971) Rhodopsin-like protein from the purple membrane of *Halobacterium halobium*, *Nature 233*, 149−152.
35. Zhang, R., and Somasundaran, P. (2004) Abnormal micellar growth in sugar-based and ethoxylated nonionic surfactants and their

mixtures in dilute regimes using analytical ultracentrifugation, *Langmuir 20*, 8552−8558.
36. Duschl, A., McCloskey, M. A., and Lanyi, J. K. (1988) Functional reconstitution of halorhodopsin. Properties of halorhodopsin-containing proteoliposomes, *J. Biol. Chem. 263*, 17016−17022.
37. London, E., and Khorana, H. G. (1982) Denaturation and renaturation of bacteriorhodopsin in detergents and lipid-detergent mixtures, *J. Biol. Chem. 257*, 7003−7011.
38. Marti, T., Rosselet, S. J., Otto, H., Heyn, M. P., and Khorana, H. G. (1991) The retinylidene Schiff base counterion in bacteriorhodopsin, *J. Biol. Chem. 266*, 18674−18683.
39. Fischer, U. C., Towner, P., and Oesterhelt, D. (1981) Light induced isomerisation, at acidic pH, initiates hydrolysis of bacteriorhodopsin to bacterio-opsin and 9-*cis*-retinal, *Photochem. Photobiol. 33*, 529−537.
40. Zimanyi, L., and Lanyi, J. K. (1987) Iso-halorhodopsin: A stable, 9-*cis* retinal containing photoproduct of halorhodopsin, *Biophys. J. 52*, 1007−1013.
41. Pande, C., Callender, R. H., Chang, C. H., and Ebrey, T. G. (1986) Resonance Raman study of the pink membrane photochemically prepared from the deionized blue membrane of *H. halobium*, *Biophys. J. 50*, 545−549.
42. Gaertner, W., Towner, P., Hopf, H., and Oesterhelt, D. (1983) Removal of methyl groups from retinal controls the activity of bacteriorhodopsin, *Biochemistry 22*, 2637−2644.
43. Booth, P. J., and Farooq, A. (1997) Intermediates in the assembly of bacteriorhodopsin investigated by time-resolved absorption spectroscopy, *Eur. J. Biochem. 246*, 674−680.

BI0511235